Stimulated optical pumping in a Tm^{3+}:YAG crystal

Stimulated optical pumping in a Tm^{3+}:YAG crystal

G Gorju[1], **A Louchet**[1], **D Paboeuf**[1], **F Bretenaker**[1], **F Goldfarb**[1], **T Chanelière**[1], **I Lorgeré**[1], **J-L Le Gouët**[1], **O Guillot-Noël**[2] and **Ph Goldner**[2]

[1] Laboratoire Aimé Cotton, CNRS-UPR 3321, Bâtiment 505, Campus d'Orsay, F-91405 Orsay Cedex, France
[2] Laboratoire de Chimie de la Matière Condensée de Paris, CNRS-UMR 7574, Ecole Nationale Supérieure de Chimie de Paris, 11, rue Pierre et Marie Curie, F-75005 Paris, France

E-mail: philippe-goldner@enscp.fr

Abstract
The possibility of using stimulated emission to improve the optical pumping of Tm^{3+} ions embedded in Tm^{3+}:YAG to the $^3F_4$ level is explored. The oscillator strengths and the frequencies of the transitions between the ground crystal field level of $^3H_4$ to the different crystal field levels of $^3F_4$ are measured at low temperature. Stimulated emission measurements at 1461 nm are performed to evaluate the optical pumping efficiency. Application to the spectral tailoring of Tm^{3+}:YAG for quantum information applications is discussed.

(Some figures in this article are in colour only in the electronic version)

1. Introduction

Rare earth ion doped crystals (REIC) offer very long coherence lifetimes. Indeed, optical coherence lifetimes up to 2.6 ms [1] have been observed. We have to differentiate the coherence from the spontaneous emission lifetimes. The spontaneous emission lifetime gives the fundamental broadening of an optical transition, whereas the coherence lifetime gives information on its homogeneous broadening. In REIC materials, on the other hand, the optical transition is also inhomogeneously broadened up to several tens of GHz [2], offering a large number of frequency channels. These features have proved to be very promising in the field of optical signal processing. The main reason is that the coherence lifetime of these materials is consistent with electronic processing, while the inhomogeneous width far exceeds the bandwidth of the fastest electronic devices. As a consequence, the use of REIC is able to cope with several applications such as spatial routing of optical beams through spatial-spectral filtering, time-domain correlation [3], and spectral analysis of broadband radio-frequency signals [4, 5].

The long coherence lifetimes and the absence of atomic motion, and therefore of Doppler shifts and diffusion, also make REIC similar to clouds of laser cooled atoms. However, in contrast with cold atomic vapors, REIC exhibit large inhomogeneous broadening. In processes such as electromagnetically induced transparency (EIT), an attractive protocol for slow light and quantum storage applications [6], the active centers should all undergo the same interaction with the coupling field. Only atoms at Rabi frequency distance from the laser line can satisfy this condition. Extremely high intensity would be required to overcome tens of GHz inhomogeneous width, given the smallness of the oscillator strength. One can circumvent this issue by selecting the spectral group of atoms we want to make interact with the driving fields. All the other atoms shall be stowed on a long lifetime shelving state with the help of an auxiliary optical excitation.

Let us list the required levels in an EIT experiment. The EIT process itself involves two ground state sublevels, connected to a common upper electronic level by optical transitions. In addition to this Λ-shape level system one needs a long lifetime storage state. These requirements are satisfied in Eu^{3+} and Pr^{3+} doped crystals that exhibit three hyperfine sublevels in the ground state. With the help of a hyperfine shelving state, one can isolate a spectral subset of ions for hours [7–9]. However, only dye lasers are available at Eu^{3+} and Pr^{3+} driving wavelength. Such sources are difficult to stabilize under 1 kHz, as requested to drive the long lifetime coherences of these ions.

We recently built a Λ system in another non-Kramers ion, namely Tm^{3+} in a YAG matrix [10–12]. Tm^{3+}:YAG is especially attractive because it presents a transition at 793 nm in the range of semiconductor lasers that can be stabilized to better than 1 kHz [13]. However, only two hyperfine sublevels are available in the electronic ground state of Tm^{3+}:YAG. The role of shelving state can be played by the metastable level $^3F_4$, but storage efficiency should be improved. In this paper we propose to stimulate the decay from the upper level $^3H_4$ to $^3F_4$ in order to accelerate the ground state depletion and the transfer to the shelving state.

The paper is arranged as follows. After a short presentation of the Tm^{3+}:YAG energy levels, we describe the stimulated transfer procedure. Section 4 is devoted to the experimental set-up. In section 5, we investigate the emission spectrum between the multiplets $^3H_4$ and $^3F_4$ to predict which transition is the most adequate. In section 6, we perform stimulated emission experiments and estimate the efficiency of this new method.

2. Structure and energy levels of Tm^{3+}:YAG

The YAG crystal has a cubic garnet structure corresponding to the space group $Ia3d$. Tm^{3+} ions mainly substitute Y^{3+} ions in the structure and are located in sites of D_2 point symmetry. These sites are repeated six times in each unit cell through the crystal point group operations. Each site has a different orientation with respect to the cell axes, which is especially important in the presence of an external magnetic field [11]. In cubic systems, emission or absorption intensities are independent of the polarization and propagation directions, assuming that the six sites are randomly occupied by the optically active ions. In D_2 point symmetry, electric and magnetic dipole transitions obey the same selection rule: transitions occurring between levels having the same irreducible representation are forbidden ($\Gamma_i \nrightarrow \Gamma_i$).

Complete energy level schemes for Tm^{3+} in YAG and crystal field (CF) calculations have been reported in [14] and [15]. Retrieving CF levels from experiments is quite difficult since no polarized emission can be recorded and some transitions are broadened by phonon coupling. Moreover, lines corresponding to perturbed sites are also observed and can mask the main site weak lines [15]. This may explain the differences in the energy levels (position and irreducible representations) proposed in the papers quoted above.
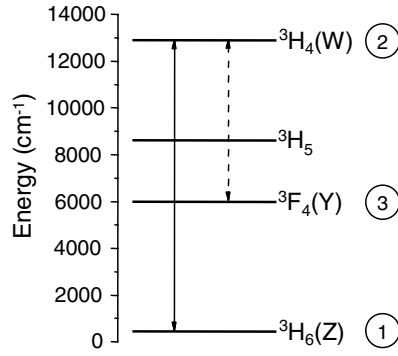
Figure 1. Lower energy levels of Tm^{3+} and labels used in the text. Thick arrow: writing/reading transition at 793 nm, dashed arrow: emptying transition at 1.461 μm.

Figure 1 represents the lower energy levels of Tm^{3+}:YAG. In this paper we note Z_i, W_i, Y_i the CF levels of the multiplets $^3H_6$, $^3H_4$ and $^3F_4$. For the lowest CF levels, we use $i = 1$. The $Z_1 \rightarrow W_1$ transition at 793 nm exhibits an inhomogeneous linewidth equal to 20 GHz. Besides, at low temperature (5 K) and relatively low Tm^{3+} (0.5 at.%) ion concentration, the homogeneous linewidth is equal to 150 kHz. The excited state lifetime is about 500 μs. A large part of the $^3H_4$ population ends up in $^3F_4$ by passing through the $^3H_5$ state that presents a very short lifetime. The level metastable level $^3F_4$ has a lifetime of the order of 10 ms.

3. Principle of operation

In order to completely deplete the ground state, one can optically pump the ions to the metastable state $^3F_4$. The time evolution of the population of this level is governed by:

$$\dot{n}_3(t) = \kappa_{23}n_2(t) - \kappa_{31}n_3(t), \tag{1}$$

where $n_1(t)$, $n_2(t)$, $n_3(t)$ respectively represent the population in the fundamental, excited and metastable levels, whcih are, respectively, denoted by Z_1, W_1 and Y_1. κ_{23} holds for the relaxation rate from $^3H_4$ to $^3F_4$ and κ_{31} is the relaxation rate from the metastable to the ground state. In the steady state, we obtain:

$$n_3 = \frac{\kappa_{23}}{\kappa_{31}}n_2. \tag{2}$$

By exciting the optical transition $Z_1 \rightarrow W_1$, one can equalize the populations $n_1(t)$ and $n_2(t)$. By considering $n_1 + n_2 + n_3 = 1$, we can write:

$$n_1 = n_2 = \frac{\kappa_{31}}{2\kappa_{31} + \kappa_{23}} \tag{3}$$

and

$$n_3 = \frac{\kappa_{23}}{2\kappa_{31} + \kappa_{23}}. \tag{4}$$

Thus, the ratios n_3/n_1 and n_3/n_2 are ultimately limited by the ratio κ_{23}/κ_{31}. In the case of Tm^{3+}, we have $\kappa_{23}/\kappa_{31} \approx 20$. Thus, around 90% of the ions can be stored in the metastable state and around 5% remain in the fundamental state and excited state. In order to store more ions in the metastable level, the ratio κ_{23}/κ_{31} has to be increased.

The relaxation rate κ_{23} can be increased by stimulating the optical transition $^3H_4 \rightarrow ^3F_4$. However, stimulated emission from the upper level should not be counteracted by adverse

absorption from the lower state of the transition. Therefore this lower level should be kept empty. Obviously this condition cannot be satisfied by the transition $W_1 \rightarrow Y_1$ since we precisely want to store the atoms in level Y_1. Consequently, we have to work with some higher Stark sublevel Y_i ($i \geqslant 2$). The multiplet $^3F_4$ is composed of nine Stark sublevels Y_i with a 75 cm^{-1} average splitting. Because of phonon relaxations, the levels Y_i ($i \geqslant 2$) have a very short lifetime and their population can be completely neglected. As a consequence, the absorption from Y_i to W_1 can also be neglected. The transition wavelengths $W_1 \rightarrow Y_i$ lie between 1.45 and 1.57 μm. Fortunately, this spectral domain corresponds to the telecom window, where some laser sources are available. By exciting the transitions $W_1 \rightarrow Y_i$, in the steady state, population n_1 becomes:

$$n_1 = \frac{\kappa_{31}}{2\kappa_{31} + \kappa_{23} + \Gamma_s}, \tag{5}$$

where Γ_s represents the probability of the $W_1 \rightarrow Y_i$ stimulated emission process.

To check the feasibility of this process, we study the $W_1 \rightarrow Y_i$ spontaneous emission spectrum to attribute all the lines to the corresponding transitions between CF levels and estimate the oscillator strengths. Then, we measure the $W_1 \rightarrow Y_i$ transitions linewidths by performing stimulated emission experiments. Thus, by calculating the probability of stimulated emission of each transition $W_1 \rightarrow Y_i$, one can predict the efficiency of the Tm^{3+}:YAG ground state depletion.

4. Experiment

All absorption and spontaneous emission experiments have been done in the Laboratoire de Chimie de la Matière Condensée de Paris. They have been performed at low temperature using a Helix closed cycle helium cryostat (sample temperature: 12 K). We perform the experiment on a 0.5 at.% thulium doped YAG crystal. Absorption spectra are measured with a Varian Cary 5 spectrophotometer. A Jobin-Yvon HRD1 600 mm double monochromator is used to record the emission spectra. Luminescence is detected by a Ge photodiode (North-Coast EO-817) connected to a Perkin-Elmer 5210 lock-in amplifier. The emission set-up is carefully calibrated in wavelength using a neon spectral lamp, resulting in a precision of ± 1 Å in the line peak positions. The response of the system is determined as a function of the wavelength with an Oriel calibrated halogen lamp. Excitation is provided by a Ti–Sa laser (Coherent 890) pumped by an argon ion laser (Coherent Sabre).

The stimulated emission experiment is performed with the set-up presented in figure 2 on a 0.5 at.% thulium doped YAG crystal. All the measurements have been done in the Laboratoire Aimé Cotton by using a cryostat with a liquid helium tank. Thanks to this cryogenic system, one can perform experiments at much lower temperatures (sample temperature: 4.5 K). We measure the gain, through the Tm^{3+}:YAG crystal, of a laser working around 1.45 μm. The laser source has been completely designed and built in the Laboratoire Aimé Cotton. Because it is an external cavity laser diode, we can tune its frequency in the range 1.4–1.5 μm to measure the linewidth of each transition. After the crystal, the laser beam is focused on a Thorlabs photodetector (PDA255) connected to a lock-in amplifier. To avoid saturation of the detector, we use neutral density filters. Another external cavity diode laser, operating at 793 nm, is used as an optical pump to excite the transition $Z_1 \rightarrow W_1$. The pump laser presents also fast frequency chirping capabilities thanks to an intra cavity electro-optic crystal [16]. It is amplitude modulated by a chopper at 40 Hz and delivers 25 mW at the sample. The mechanical chopper frequency is used to drive the lock-in amplifier. Thus, when the pump is on, one can measure optical gain for the 1.45 μm laser. Because we use an extended
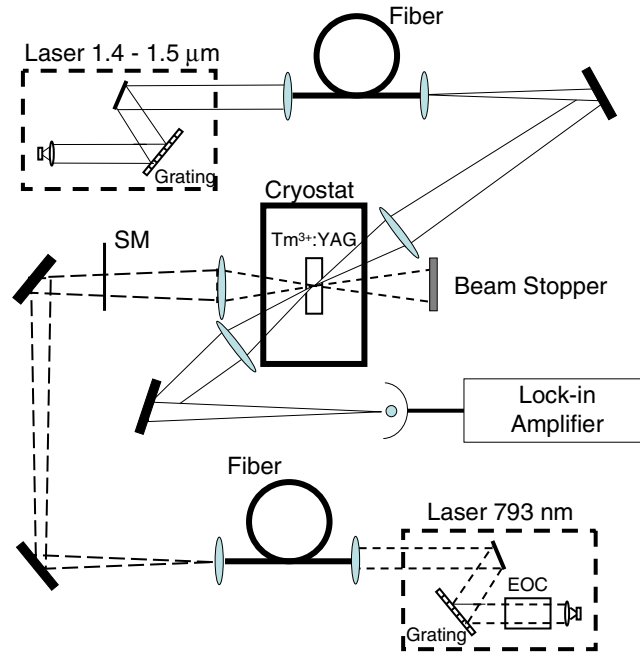
Figure 2. Experimental set-up to measure the transition $Y_1 \rightarrow W_i$. The Tm^{3+}:YAG crystal is cooled at 4.5 K. SM: spatial modulator; EOC: intracavity electro-optic crystal.

cavity configuration, the pump laser can be tuned to excite different frequency ranges of the inhomogeneous linewidth of the $Z_1 \rightarrow Y_1$ transition. In order to work with TEM_{00} laser beams, optical monomode fibers are used for spatial filtering. The pump and the probe beams are focused on the crystal to a 200 μm ($1/e^2$ diameter) spot.

Both extended cavity diode lasers present a spectral linewidth of about 1 MHz. During the experiment, the pump laser is repeatedly scanned over a 2.5 GHz bandwidth at 1 kHz around its average frequency. Chirping the laser allows us to work with more atoms, hence increasing the signal to noise ratio of our experiment. The pump laser frequency and amplitude modulations are asynchronous.

5. Low temperature spectroscopy

To confirm that the samples are really at 12 K under our experimental conditions, we checked that no hot bands appear in low temperature excitation and emission spectra when a low excitation laser power was used (10 to 20 mW). As a result, all emissions from the $^3H_4$ multiplet started from the W_1 CF level. We also compared $^3H_4 \rightarrow {}^3H_6$ emission spectra in the 0.5 and 4 at% Tm^{3+}:YAG samples. Since the spectra had similar shapes and relative intensities, we concluded that reabsorption effects were negligible for the $W_1 \rightarrow Z_1$ transition.

5.1. $^3H_4 \rightarrow {}^3H_6$ and $^3H_4 \rightarrow {}^3F_4$ emissions

The $^3H_4 \rightarrow {}^3H_6$ emission spectrum obtained at low temperature is presented in figure 3. We first analyse it by comparing the line positions with the energy levels given in [15], which were either experimentally determined, or calculated by CF theory. We observed three intense lines
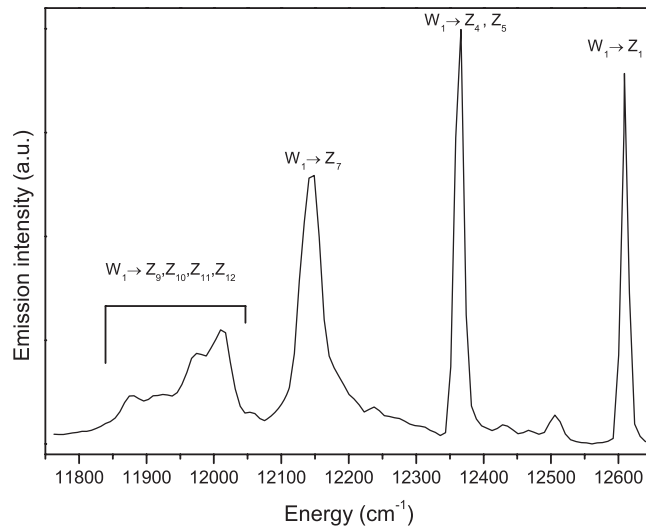
Figure 3. $^3H_4 \rightarrow\ ^3H_6$ emission at 12 K excited at 784.7 nm.

at 12 608, 12 366 and 12 145 cm^{-1} which are attributed to the $W_1 \rightarrow Z_1$, $W_1 \rightarrow Z_4, Z_5$ and $W_1 \rightarrow Z_7$ transitions. The positions of the two high energy lines are located within 2 cm^{-1} of those deduced in [15], in agreement with the precision of our monochromator. On the other hand, the broader transition centered at 12 145 cm^{-1} is 13 cm^{-1} lower than the position measured in [15]. However, the position calculated from the CF analysis is 12 146 cm^{-1}. Several broad peaks are also observed between 11 850 and 12 045 cm^{-1} and correspond to the $W_1 \rightarrow Z_9, Z_{10}, Z_{11}, Z_{12}$ transitions. The two lines at the lowest energies (11 876 and 11 923 cm^{-1}) are in good agreement with the levels measured in [15]. In contrast, the two other lines at 11 974 and 12 012 cm^{-1} are 10–15 cm^{-1} too low. As mentioned above, this can be explained by phonon sidebands or minority site lines. According to the irreducible representations determined or calculated for the CF levels of the $^3H_4$ and $^3H_6$ multiplets and the D_2 point symmetry, all allowed transitions are observed except for $W_1 \rightarrow Z_3$.

Comparing our results with the energy scheme reported in [14], we found a more significant discrepancy because these authors did not give any $^3H_6$ CF level around 460 cm^{-1}. Accordingly, the intense line observed at 12 144 cm^{-1} cannot be attributed to any $W_1 \rightarrow Z_i$ transition. We also checked that no transition from the W_2 CF level (12 679 cm^{-1} in [14]) could correspond to this line.

The $^3H_4 \rightarrow\ ^3F_4$ emission spectrum (figure 4) shows five strong lines at 6844, 6772, 6704, 6495 and 6432 cm^{-1}. These energies are in very good agreement with the experimental levels reported in [15], with a maximum difference of 3 cm^{-1}. Attributions of the lines to transitions between CF levels are given in figure 4. Out of the six allowed transitions, only $W_1 \rightarrow Y_9$ is not observed at 6408 cm^{-1}. As in the case of the $^3H_4 \rightarrow\ ^3H_6$ transition, our data do not completely agree with the levels given in [14] as the line at 6495 cm^{-1} should not be observed because of the $\Gamma_i \nrightarrow \Gamma_i$ selection rule.

5.2. Emission intensity calculations

To determine the oscillator strengths around 1.5 μm, we used the $W_1 \leftrightarrow Z_1$ transition which is observed both in emission and absorption. Then, relative emission intensities allowed us to
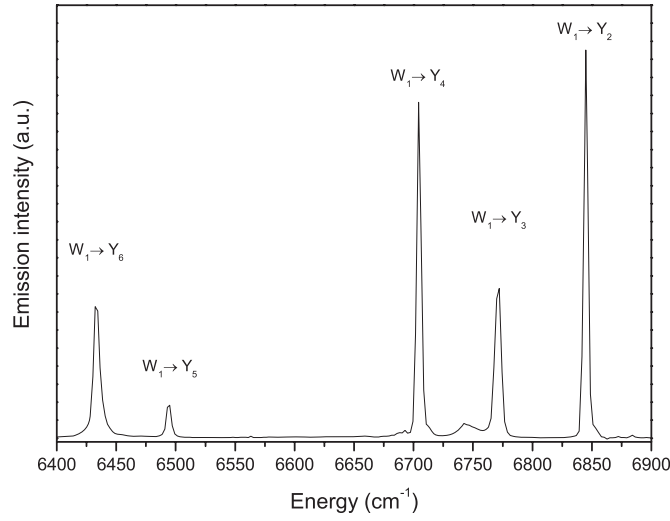
Figure 4. $^3H_4 \to \ ^3F_4$ emission at 12 K excited at 784.7 nm.

obtain the absolute values for all other transitions. Since the emission and absorption intensities were quite low, it was not possible to use a spectrometer resolution suitable to faithfully record narrow lines. For example, the $W_1 \to Z_1$ transition has an inhomogeneous linewidth of $\approx$20 GHz or 0.4 Å. To ensure a good signal to noise ratio, we used rather low resolutions for emission (0.6 Å) and absorption (0.2 Å) spectra and only determined integrated emission intensities. The latter were finally used to normalize the $W_1 \to Y_2$ stimulated emission spectrum obtained with the narrow linewidth laser diode ($\approx$1 MHz) at 1461.1 nm, allowing us to obtain the true wavelength dependent oscillator strengths (see section 6).

The oscillator strength of the $Z_1 \to W_1$ transition was determined from the absorption spectrum at 12 K using the formula:

$$f = \frac{4\epsilon_0 m c^2}{Ne^2} \int \alpha(\overline{\nu}) \, d\overline{\nu}, \tag{6}$$

where ϵ_0 is the vacuum electric permittivity, m and e the electron mass and charge, c the speed of light, N the Tm^{3+} concentration (in ions m^{-3}), α the absorption coefficient and $\overline{\nu}$ the wavenumber (in m^{-1}). Taking into account a 0.96 distribution coefficient, the 0.5 at.% Tm^{3+} nominal concentration of the sample corresponds to 6.64×10^{19} ions cm^{-3}, giving an oscillator strength of $f(Z_1 \to W_1) = 1.15 \times 10^{-7}$. This value is in agreement with the one determined for a 0.1 at.% Tm^{3+}:YAG sample at 1.4 K: 1.30×10^{-7} [17]. The 12% discrepancy can be due to differences in actual Tm^{3+} concentration in the crystals and to the measurement temperature (1.4 K versus 12 K).

The ratio between oscillator strengths of transitions originating from the same CF level is given by:

$$\frac{f(i \to j)}{f(i \to k)} = \frac{I(i \to j)}{I(i \to k)} \frac{\overline{\nu_m(i \to j)}}{\overline{\nu_m(i \to k)}} \tag{7}$$

where i, j, k are CF levels, I is the integrated luminescence intensity and $\overline{\nu_m}$ the average wavenumber of the transition.

Since W_1 and Z_1 are both singlets, $f(W_1 \to Z_1) = f(Z_1 \to W_1)$ and emission oscillator strengths for the $^3H_4 \to \ ^3F_4$ lines can be directly deduced from (7) and the calibrated
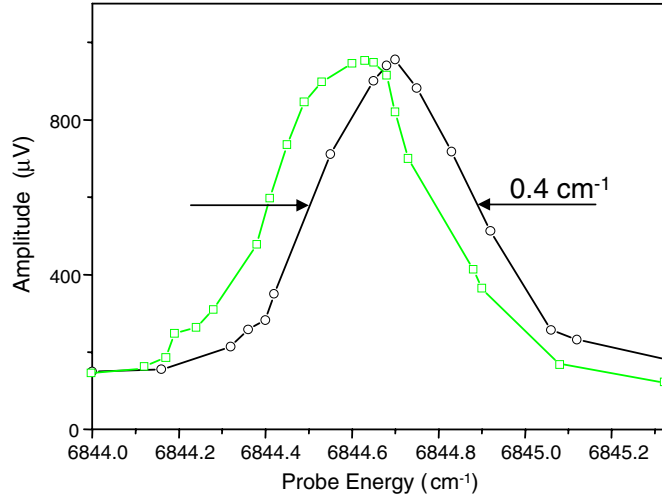
Figure 5. Stimulated emission profile of the transition $W_1 \rightarrow Y_2$ obtained for two different average pump laser frequencies. Open squares: the pump laser average frequency corresponds to an energy of $12\,604.62$ cm^{-1}. Open circles: the pump laser average frequency corresponds to an energy of $12\,604.25$ cm^{-1}. Each profile has a FWHM of 0.4 cm^{-1}.

Table 1. Oscillator strengths f of $^3H_4 \rightarrow {}^3F_4$ emission lines in Tm^{3+}:YAG.

Transition	Mean energy (cm^{-1})	$f \times 10^8$
$W_1 \rightarrow Y_2$	6844	4.1
$W_1 \rightarrow Y_3$	6772	2.1
$W_1 \rightarrow Y_4$	6704	3.7
$W_1 \rightarrow Y_6$	6495	0.65
$W_1 \rightarrow Y_8$	6432	3.5

emission spectra. The values are gathered in table 1. Oscillator strengths for the $W_1 \rightarrow Y_i$ emissions are at least 35% lower than the $W_1 \rightarrow Z_1$ one. This behavior is similar to those of the mean electric dipole oscillator strengths which can be evaluated by the Judd–Ofelt theory [18, 19]. Using the Judd–Ofelt coefficients $\Omega_2 = 0.89 \times 10^{-20}$, $\Omega_4 = 1.08 \times 10^{-20}$, $\Omega_6 = 0.68 \times 10^{-20}$ for Tm^{3+}:YAG [20] and the corresponding reduced matrix elements [21], we found $f(^3H_4 \rightarrow {}^3H_6) = 1.8 \times 10^{-6}$ and $f(^3H_4 \rightarrow {}^3F_4) = 5.8 \times 10^{-7}$.

These calculations suggest that the $W_1 \rightarrow Y_2$ line is the most adequate to empty the $^3H_4$ population through stimulated emission; it is one of the strongest lines in the $^3H_4 \rightarrow {}^3H_6$ transition and occurs at a wavelength (1461.1 nm) for which our laser diode nearly reaches its maximum output power. It is important to note that our laser cannot be tuned at wavelengths longer than 1490 nm (6711 cm^{-1}) meaning, for example, that the $W_1 \rightarrow Y_4$ transition cannot be excited.

6. Stimulated emission

The stimulated emission spectra of the transition $W_1 \rightarrow Y_2$, performed with the set-up presented in figure 2, are displayed in figure 5. The results have been obtained for two different pump laser average frequencies. The open circles and squares respectively correspond to a pump laser average frequency of $12\,604.25$ and $12\,604.62$ cm^{-1}. For this experiment, the

probe laser has been tuned between 6844 and 6845.3 cm^{-1}. One notices a spectral shift of 0.07 cm^{-1} (2.7 GHz) between the two spectra. It means that there is a correlation between the inhomogeneous broadenings of transitions $Z_1 \rightarrow W_1$ and $W_1 \rightarrow Y_2$. Nevertheless, we cannot precisely estimate this inhomogeneous broadening.

By measuring the full width at half maximum (FWHM) of the spectrum, we find $\Delta \nu \approx$ 0.4 cm^{-1} (11 GHz). We notice that the $W_1 \rightarrow Y_2$ optical transition linewidth is much larger than the excited spectral region (2.5 GHz) showing that the transition can be considered as mainly homogeneously broadened. Furthermore, we have checked that the widths of the spectra are independent of the amplitude of the pump laser frequency scan. The relatively large linewidth of the studied transition is probably due to non-radiative processes. By performing the same experiment at 1.5 and 30 K, we have noticed a very weak temperature dependence of the linewidth.

As mentioned before, the transitions $W_1 \rightarrow Y_i$ with $i = \{6, 5, 4\}$ have not been measured because the laser cannot be tuned at energies smaller than 6720 cm^{-1}. Concerning the transition $W_1 \rightarrow Y_3$, we were not able to measure any stimulated emission. This is not really surprising, knowing that the oscillator strength of this transition has been estimated at around 2.1×10^{-8}.

Thus, only the transition $W_1 \rightarrow Y_2$ can be used to increase the Tm^{3+}:YAG ground state depletion efficiency. Since the homogeneous broadening is predominant, one can write the transition probability due to stimulated emission:

$$\Gamma_s(\nu) = f A I g(\nu - \nu_0), \tag{8}$$

where $A = (e^2)/(4h\epsilon_0 m\nu_0 c)$, I is the laser beam optical intensity, ν_0 is the center frequency of the considered transition, $g(\nu - \nu_0)$ is the homogeneous profile which is supposed to be Lorentzian and $\Delta \nu$ is the FWHM of the considered transition. Thus by using an external cavity diode laser presenting a narrow linewidth and centered at ν_0, the previous equation becomes:

$$\Gamma_s(\nu_0) = f \frac{2A}{\pi \Delta \nu} I. \tag{9}$$

Thus, in steady state, the ground state population is given by:

$$n_1 = \frac{\kappa_{31}}{2\kappa_{31} + \kappa_{23} + f \frac{2A}{\pi \Delta \nu} I}. \tag{10}$$

To obtain a significant stimulated emission effect, one needs to satisfy the condition:

$$\Gamma_s \geqslant \kappa_{23}. \tag{11}$$

Consequently the optical intensity must satisfy the condition

$$I \geqslant \frac{\kappa_{23} \pi \Delta \nu}{2Af}. \tag{12}$$

By considering a spot diameter of 200 μm, one needs an optical power of around 2 W to observe a significant improvement of the ground state emptying efficiency. This is not realizable with a simple external cavity diode laser. However, by using beam waists of 10 μm, the needed power is reduced down to 20 mW, which is feasible. To have a beam waist of 10 μm, one should use a lens of very short focal length in front of the cryostat. However, we cannot realize this experiment because we were limited by the distance separating the crystal and the cryostat windows.

7. Conclusion

In conclusion, we have investigated a technique to isolate a spectrally narrow absorptive feature in the inhomogeneously broadened $^3H_6 \rightarrow {}^3H_4$ transition in Tm^{3+}:YAG. In contrast with the

standard experiment realized in Eu^{3+}, we used, as a shelving state, an energy level presenting a relatively short lifetime. The paper shows that by using stimulated emission around 1.5 μm for the transitions $^3H_4 \rightarrow \, ^3F_4$ one can improve the emptying efficiency of the the ground state. Indeed, we show that five different absorption lines lying in the telecom window can be potentially used. For the transition $Y_1 \rightarrow W_2$, we have estimated the probability of stimulated emission and conclude that it is possibile to prepare an isolated narrow absorptive spectral feature in a system presenting a relatively short lifetime shelving state. We plan to realize some coherent process experiments in Tm^{3+}:YAG as EIT. Thus, the use of laser sources stabilized better than 1 MHz, opens new and interesting perspectives.

Acknowledgment

References

[1] Equall R W, Sun Y, Cone R L and Macfarlane R M 1997 *Phys. Rev. Lett.* **44** 2179
[2] Equall R W, Sun Y, Cone R L and Macfarlane R M 2002 *J. Lumin.* **98** 281
[3] Harris T L, Sun Y, Cone R L, Macfarlane R M and Equall R W 2000 *Opt. Lett.* **25** 85
[4] Gorju G, Crozatier V, Lorgeré I, Le Gouët J L and Bretenaker F 2005 *IEEE J. Photon. Technol. Lett.* **17** 2385
[5] Gorju G, Chauve A, Crozatier V, Lorgeré I, Le Gouët J L and Bretenaker F 2007 *J. Opt. Soc. Am.* B **24** 457
[6] Turukhin A V, Sudarshanam V S, Shahriar M S, Musser J A, Ham B S and Hemmer P R 2002 *Phys. Rev. Lett.* **88** 023602
[7] Pryde G Y, Sellars M J and Manson N B 2000 *Phys. Rev. Lett.* **84** 1152–5
[8] Nilsson M, Rippe L, Kroll S, Klieber R and Suter D 2004 *Phys. Rev.* B **70** 214116
[9] Yano R, Mitsunaga M and Uesugi N 1991 *Opt. Lett.* **16** 1884–6
[10] de Seze F, Louchet A, Crozatier V, Lorgeré I, Bretenaker F, Le Gouët J L, Guillot-Noël O and Goldner P 2006 *Phys. Rev.* B **73** 85112
[11] Guillot-Noël O, Goldner P, Antic-Fidancev E and Le Gouët J L 2005 *Phys. Rev.* B **71** 174409
[12] Louchet A, Habib J S, Crozatier V, Lorgeré I, Goldfarb F, Bretenaker F, Le Gouët J L, Guillot-Noël O and Goldner P 2007 *Phys. Rev.* B **75** 035131
[13] Crozatier V, de Seze F, Haals L, Bretenaker F, Lorgeré I and Le Gouët J L 2004 *Opt. Commun.* **241** 203–13
[14] Gruber J B, Hills M E, Macfarlane R M, Morrison C A, Turner G A, Quarles G J, Kintz G J and Esterowitz L 1989 *Phys. Rev.* B **40** 9464–78
[15] Tiseanu C, Lupei A and Lupei V 1995 *J. Phys.: Condens. Matter* **7** 8477–86
[16] Ménager L, Cabaret L, Lorgeré I and Le Gouët J L 2000 *Opt. Lett.* **25** 1246
[17] Sun Y, Wang M and Cone R L 2004 *Phys. Rev.* **62** 15443
[18] Judd B 1962 *Phys. Rev.* B **127** 750–61
[19] Ofelt G 1962 *J. Chem. Phys.* **37** 511
[20] Antipenko B M and Tomashevich Y V 1978 *Opt. Spectrosc.* **44** 157
[21] Spector N, Reisfeld R and Boehm L 1977 *Chem. Phys. Lett.* **49** 49–53